Hybrid incompatibility caused by an epiallele

Todd Blevins[a,b,1,2,3], Jing Wang[b,1], David Pflieger[c], Frédéric Pontvianne[b,4], and Craig S. Pikaard[a,b,d,3]

[a]Howard Hughes Medical Institute, Indiana University, Bloomington, IN 47405; [b]Department of Biology, Indiana University, Bloomington, IN 47405; [c]Institut de Biologie Moléculaire des Plantes, CNRS UPR2357, Université de Strasbourg, F-67084 Strasbourg, France; and [d]Department of Molecular and Cellular Biochemistry, Indiana University, Bloomington, IN 47405

Hybrid incompatibility resulting from deleterious gene combinations is thought to be an important step toward reproductive isolation and speciation. Here, we demonstrate involvement of a silent epiallele in hybrid incompatibility. In *Arabidopsis thaliana* accession Cvi-0, one of the two copies of a duplicated histidine biosynthesis gene, *HISN6A*, is mutated, making *HISN6B* essential. In contrast, in accession Col-0, *HISN6A* is essential because *HISN6B* is not expressed. Owing to these differences, Cvi-0 × Col-0 hybrid progeny that are homozygous for both Cvi-0 *HISN6A* and Col-0 *HISN6B* do not survive. We show that *HISN6B* of Col-0 is not a defective pseudogene, but a stably silenced epiallele. Mutating *HISTONE DEACETYLASE 6* (*HDA6*), or the cytosine methyltransferase genes *MET1* or *CMT3*, erases *HISN6B*'s silent locus identity, reanimating the gene to circumvent *hisn6a* lethality and hybrid incompatibility. These results show that *HISN6*-dependent hybrid lethality is a revertible epigenetic phenomenon and provide additional evidence that epigenetic variation has the potential to limit gene flow between diverging populations of a species.

gene silencing | epigenetic inheritance | DNA methylation | histone deacetylation | hybrid incompatibility

Mutations that accumulate in separate subpopulations of a species can facilitate reproductive isolation by engendering hybrid incompatibility, a reduction in fitness observed among hybrid progeny at the F1 or F2 generation (1–3). Bateson (4), Dobzhansky (5), and Muller (6) independently proposed that gene mutations made benign by compensatory mutations in interacting genes within isolated subpopulations prove deleterious when subpopulations or ecotypes interbreed, thereby contributing to speciation by reducing gene flow. Examples of this include the lethal consequences of a *Saccharomyces cerevisiae* protein directing improper splicing of essential *Saccharomyces bayanus* mRNAs in *S. cerevisiae* × *S. bayanus* hybrids (3) or the hybrid necrosis that results from expression of incompatible innate immune receptors in *Arabidopsis thaliana* (1).

Lynch and Force (7) envisioned an alternative scenario by which hybrid incompatibilities might arise, as a result of gene duplication. Gene duplication initially results in gene redundancy, thereby relaxing constraints on sequence and functional divergence, but mutations most often transform one paralog into a nonfunctional pseudogene (8–10). Lynch and Force recognized that asymmetric resolution of gene duplicates in this manner could result in either paralog becoming the sole operational copy in different subpopulations of a species, such that hybrid progeny inheriting nonfunctional alleles of both subpopulations would suffer reduced fitness (7).

Nonmutational (epigenetic) gene silencing could potentially contribute to hybrid incompatibility via the scenario envisioned by Lynch and Force. In plants, silent epialleles segregating in Mendelian fashion can be stably inherited over many generations, and are known to affect a number of well-studied traits, including flower morphology (11, 12), fruit ripening (13), and sex determination (14). Silent epialleles are inherited via the perpetuation of repressive chromatin states, and various plant chromatin-modifying enzymes are known to participate in epigenetic inheritance, including the Rpd3-like histone deacetylase HDA6, the ATP-dependent chromatin remodeler DDM1, and the DNA methyltransferases MET1 and CMT3 (15–25). These enzymes are important for maintaining patterns of cytosine methylation following each round of DNA replication, such that newly replicated daughter strands of DNA inherit the methylation status of mother strands.

Multicopy transgenes frequently become methylated and silenced, particularly when inserted into the genome as inverted repeats that can give rise to double-stranded RNAs (26). Such double-stranded RNAs can be diced into small interfering RNAs (siRNAs) that guide the cytosine methylation of homologous DNA sequences, a process known as RNA-directed DNA methylation (RdDM) (27, 28). Known cases of silencing that involve duplicated endogenous genes, such as the phosphoribosylanthranilate isomerase (*PAI*) or folate transporter (*AtFOLT*) genes of *A. thaliana*, resemble transgene silencing in that complex sequence rearrangements coincide with duplication of a gene to create a novel (nonancestral) locus engendering siRNA production and homology-dependent DNA methylation (29, 30). Silencing of the ancestral *AtFOLT1* gene, directed by siRNAs derived from the novel *AtFOLT2* locus present in some ecotypes, causes reduced fertility in ecotype-specific hybrid combinations (29). This interesting case study has shown that naturally occurring RdDM, involving a new paralog that inactivates the ancestral paralog in *trans*, can be a cause of hybrid incompatibility.

Here, we demonstrate an epigenetic basis for a previously identified case of hybrid incompatibility (31) involving a gene pair, *HISN6A* and *HISN6B*. The underlying mechanism of *HISN6*-based hybrid incompatibility was previously unknown. We show that the *HISN6B* gene of ecotype Col-0, and hundreds of other *A. thaliana* natural accessions, is hypermethylated in its promoter region and is epigenetically silent, making its paralog, *HISN6A*, essential. Inheritance of the silent *HISN6B* epiallele

Significance

Deleterious mutations in different copies of a duplicated gene pair have the potential to cause hybrid incompatibility between diverging subpopulations, contributing to reproductive isolation and speciation. This study demonstrates a case of epigenetic gene silencing rather than pseudogene creation by mutation, contributing to a lethal gene combination on hybridization of two ecotypes of *Arabidopsis thaliana*. Our findings provide direct evidence that naturally occurring epigenetic variation can contribute to incompatible hybrid genotypes, reducing gene flow between subtypes of the same species.

requires HDA6-, MET1-, and CMT3-dependent cytosine methylation, but is unaffected by mutations disrupting RdDM. Although methylated *HISN6B* epialleles can be stably inherited for at least 30 generations, they can revert to an active state if the epigenetically silent state is erased by passage through an *hda6* mutant background. This allows *HISN6B* to now rescue *hisn6a* null mutations in ecotype Col-0 and to restore compatibility with ecotype Cvi-0, in which *HISN6A* is defective owing to an internal deletion. Collectively, our results demonstrate that *HISN6*-dependent hybrid lethality is a previously unrecognized epigenetic phenomenon.

Results

HISN6A and *HISN6B* are duplicated, paralogous genes (Fig. 1*A* and Fig. S1) encoding histidinol-phosphate aminotransferase, which converts imidazole-acetol phosphate to histidinol-phosphate in the histidine biosynthesis pathway (32, 33) (Fig. 1*B*). The gene duplication occurred after *A. thaliana* diverged from a common ancestor with *Arabidopsis lyrata* (34, 35), resulting in duplication of a segment of chromosome 1 containing *HISN6B* (At1g71920) on chromosome 5, yielding the *HISN6A* locus, At5g10330 (33, 36). Although *HISN6A* and *HISN6B* coding regions are 100% identical at the amino acid level, homozygous *hisn6a* null mutations are embryo-lethal in ecotype Col-0, because *HISN6B* is not expressed (Fig. 1 *B* and *C*) (31, 32). This differential expression of *HISN6A* and *HISN6B* can be observed by RT-PCR amplification followed by digestion with RsaI, which cuts only *HISN6A* cDNA (Fig. 1*C*). In wild-type (WT) Col-0, only *HISN6A* is expressed (Fig. 1*D*); however, in *hda6-6* or *hda6-7* mutants (37, 38), *HISN6B* is expressed as well (Fig. 1*D*), which is also true in mutants for *MET1* or *CMT3*, which encode enzymes responsible for cytosine maintenance methylation
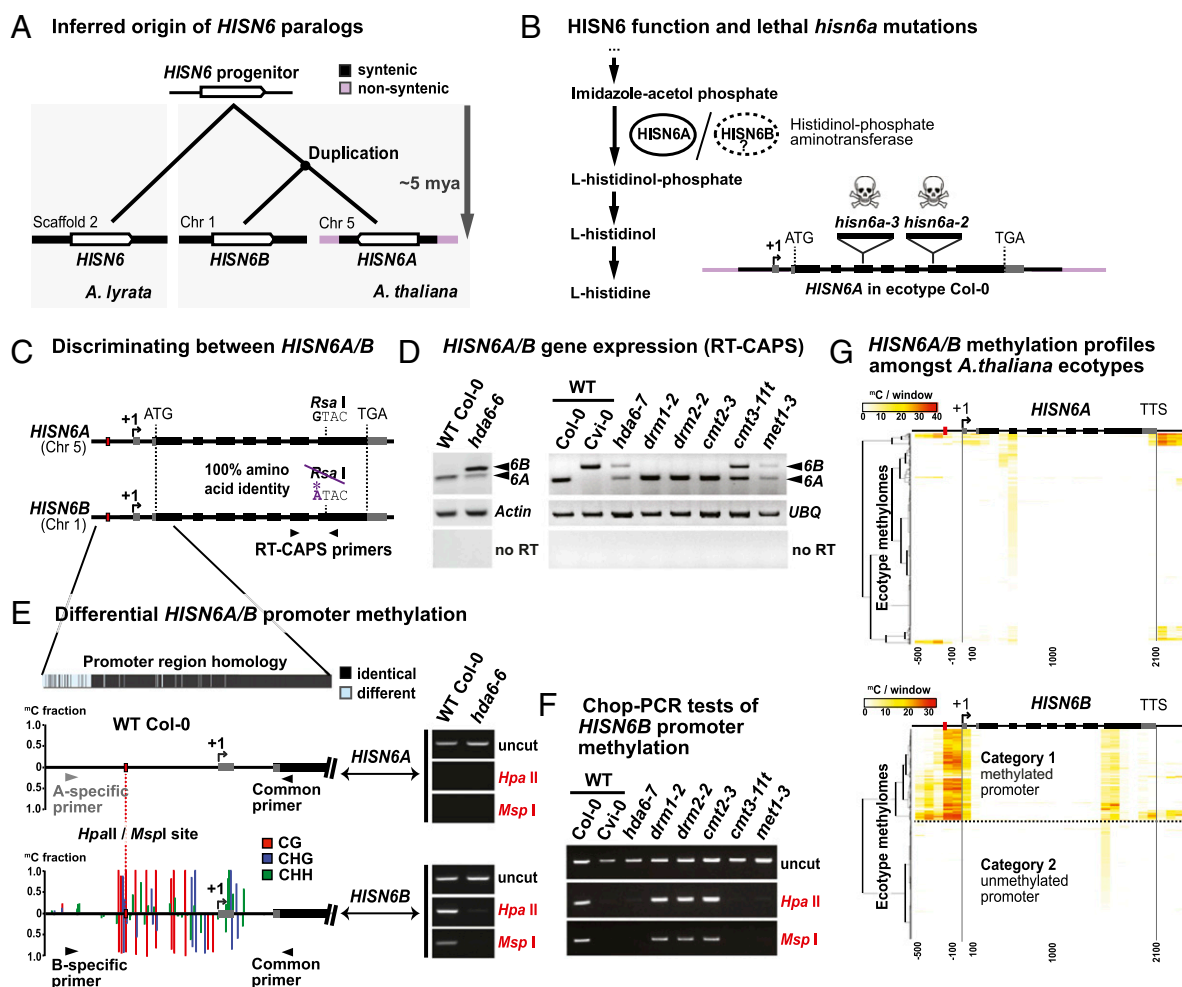

Fig. 1. HDA6, CMT3, and MET1 silence *HISN6B* via promoter region DNA methylation. (*A*) Inferred phylogenetic origin of *HISN6* paralogs based on synteny between *HISN6B* flanking regions on *A. thaliana* chromosome 1 and sequences including the single copy *HISN6* gene of *A. lyrata* scaffold 2 (Fig. S1 *A* and *B*). (*B, Left*) HISN6A/B protein function in histidine biosynthesis. Steps upstream of Imidazole-acetol phosphate are omitted. (*B, Right*) Gene structure of *HISN6A* in ecotype Col-0: UTRs, exons, and T-DNA insertion positions in mutant alleles are indicated by gray boxes, black boxes, and inverted triangles, respectively. (*C*) RT-CAPS assay for discrimination of *HISN6A* and *HISN6B* mRNAs using primers flanking a polymorphic RsaI site present only in *HISN6A*. (*D*) *HISN6A/B* expression analysis via RT-CAPS in *hda6-6*, *hda6-7*, *drm1-2*, *drm2-2*, *cmt2-3*, *cmt3-11t*, and *met1-3* mutants compared with WT Col-0 or Cvi-0. Actin and ubiquitin (*UBQ*) reactions served as loading controls. Reactions omitting reverse transcriptase (no RT) are controls for genomic DNA contamination. (*E*) Analysis of DNA methylation in *HISN6A* and *HISN6B* promoter regions. Bar plots show WT Col-0 methylation profiles, color-coded by sequence context (CG, CHG, and CHH), tabulated as fractional cytosine methylation (*y*-axis), based on methylome data of Stroud et al. (40). No methylation was detected in the *HISN6A* promoter. Gel images show Chop-PCR assays of cytosine methylation status at a *HISN6A/B* promoter HpaII/MspI site (red dotted line) in WT Col-0 or the *hda6-6* mutant. Reactions omitting restriction enzymes (uncut) demonstrate equivalent DNA input. *HISN6A/B* primer specificity was verified by sequencing PCR products. (*F*) Analysis of *HISN6B* promoter methylation in the mutant series of *D*, using Chop-PCR. (*G*) Hierarchical clustering of cytosine methylation profiles for *HISN6A* (*Top*) or *HISN6B* (*Bottom*) genes in 892 ecotype methylomes of *A. thaliana*. Methylated cytosines, based on data of Kawakatsu et al. (41), were tallied within 100-bp nonoverlapping windows starting 500 bp upstream of the transcription start site (+1) and stopping 300 bp downstream of the TTS.

in the CG and CHG sequence contexts (39), respectively (Fig. 1*D* and Fig. S2*A*). In contrast, *HISN6B* is not derepressed in mutants deficient for RNA-directed de novo cytosine methylation, such as *nrpd1-3* (Pol IV), *nrpe1-11* (Pol V), and *drm2* (Fig. 1*D* and Fig. S2*A*).

HISN6 promoter CG and CHG methylation is easily assayed using Chop-PCR, a test in which genomic DNA is first digested (chopped) with methylation-sensitive restriction endonuclease HpaII or MspI before PCR amplification of a region that includes a HpaII/MspI recognition site, CCGG. In our tests, we assayed a HpaII/MspI site in the promoter region (Fig. 1*E*, red dotted line), where Col-0 methylome data (40) showed that dense CG and CHG methylation and scattered CHH methylation occur in *HISN6B*, but not in *HISN6A* (Fig. 1*E* gene diagrams). Using the Chop-PCR assay, PCR products were detected for *HISN6B* (Fig. 1*E*, *Bottom Right*), but not for *HISN6A* (Fig. 1*E*, *Top Right*), indicating CG and CHG methylation of the *HISN6B* promoter CCGG site, but not of the corresponding *HISN6A* site. *HISN6B* promoter CG and CHG methylation was lost in *hda6-6*, *met1-3*, and *cmt3-11t* mutants, but not in Pol IV (*nrpd1-3*) and Pol V (*nrpe1-11*) mutants or mutants defective for the DNA methyltransferases DRM1, DRM2, or CMT2 (Fig. 1 *E* and *F* and Fig. S2 *B* and *C*). Although 24-nt siRNAs matching the *HISN6B* promoter were detected by RNA-seq (Fig. S2*D*) (15), their absence in the *nrpd1-3* mutant was not correlated with *HISN6B* reactivation. Collectively, the data of Fig. 1

D-F show that *HISN6B* silencing in Col-0 correlates with HDA6-, MET1-, and CMT3-dependent CG and CHG methylation. In ecotype Cvi-0, in which *HISN6A* has suffered a deletion mutation, *HISN6B* lacks promoter methylation (Fig. 1*F*) and is expressed (Fig. 1*D*). Analysis of publicly available methylome data (41) reveals *HISN6B* promoter hypermethylation in 43% (387 of 892 datasets) of the *A. thaliana* ecotype methylomes analyzed (Fig. 1*G* and Fig. S2*E*), suggesting that differential methylation, and likely silencing, of *HISN6B* is not unique to Col-0. The basis for the differential methylation of *HISN6B* among these accessions is unclear, however.

In Col-0, homozygous *hisn6a-2* progeny of *hisn6a-2*/*HISN6A* heterozygotes arrest as preglobular embryos (32). To test whether *HISN6B* derepression in the *hda6-7* mutant background rescues *hisn6a-2* lethality, we crossed a *hisn6a-2* heterozygote ($^{-/+}$) with homozygous *hda6-7* (Fig. 2*A*). One-half of the resulting F1 plants harbored one *hisn6a-2* mutant allele (red "a"), one functional *HISN6A* allele (black "A"), one silent *HISN6B* allele from the *hisn6a-2* parent (red "B"), and one active, derepressed *HISN6B* allele (black "B") from the *hda6-7* parent (Fig. 2*A*). Among 89 of their F2 progeny, 17 (19%) *hisn6a-2* homozygous mutant ($^{-/-}$) plants were recovered (Fig. 2*B*, red bars). In contrast, zero *hisn6a-2* ($^{-/-}$) plants were among the 64 progeny of self-fertilized *hisn6a-2* ($^{-/+}$) plants WT for HDA6 (Fig. 2*B*, black bars). Whereas WT Col-0
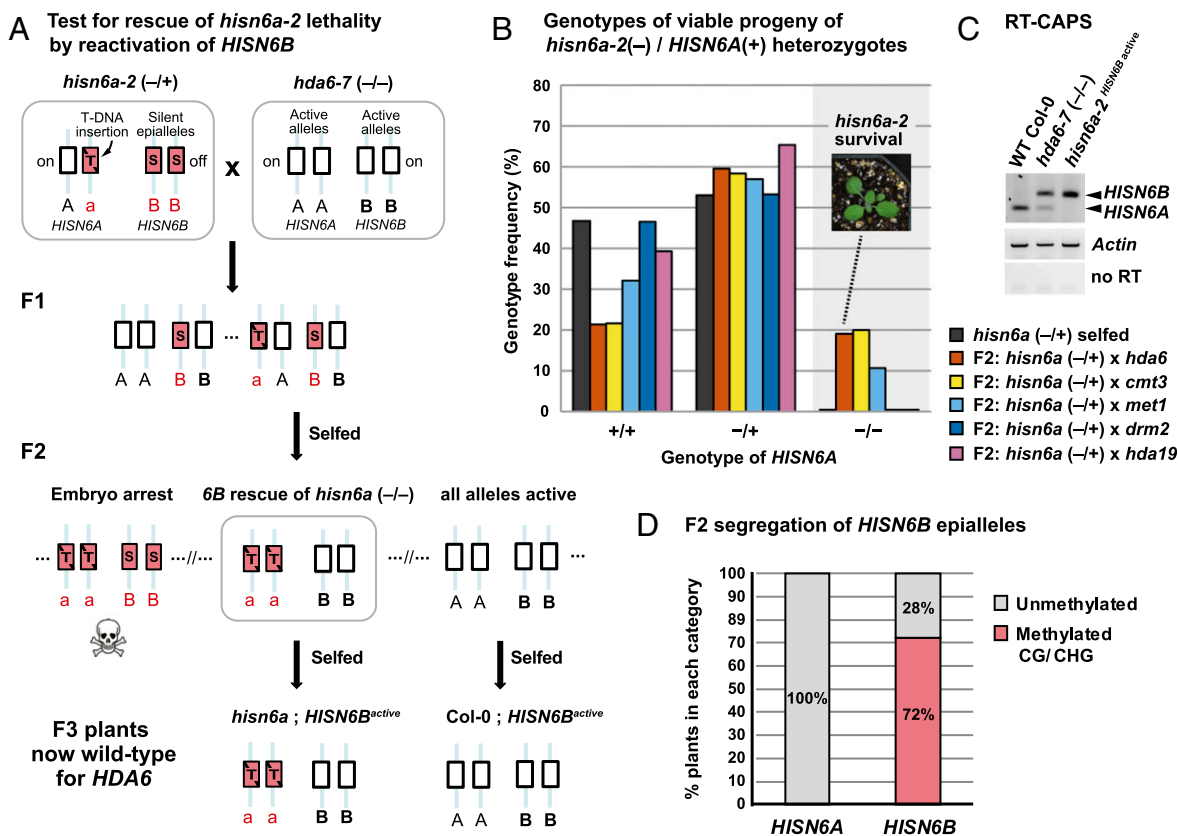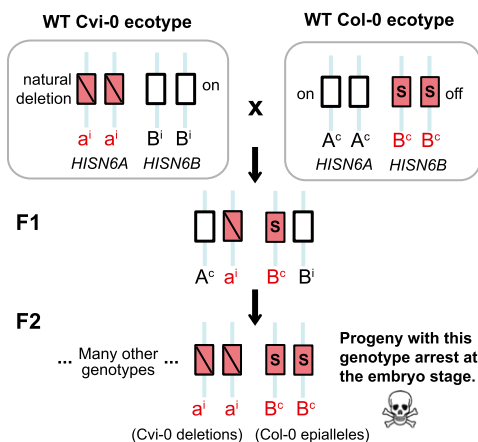

Fig. 2. Reactivating *HISN6B* via elimination of symmetric DNA methylation rescues *hisn6a-2* lethality. (*A*) Strategy for rescue of *hisn6a-2* lethality. The red "a" indicates the *hisn6a-2* null mutant allele, the red "B" indicates transcriptionally silent *HISN6B*, and the black "A" and "B" indicate transcriptionally active *HISN6A* and *HISN6B*, respectively. HDA6 genotypes are omitted for simplicity. (*B*) Tests of *hisn6a-2* rescue by passage of *HISN6B* alleles through null mutants affecting gene silencing. Heterozygous *hisn6a-2* ($^{-/+}$) was selfed (black) or crossed to *hda6-7* (orange), *cmt3-11t* (yellow), *met1-7* (light blue), *drm2-2* (blue), or *hda19-1t* (purple). Selfed *hisn6a-2* ($^{-/+}$) progeny (n = 64 plants) or F2 progeny resulting from the crosses to other mutants (n = 89, 60, 28, 60, and 30 plants, respectively) were genotyped for *hisn6a-2* and *HISN6A* alleles, the frequencies of which were plotted. (*C*) RT-CAPS analysis of *HISN6A/B* gene expression in the *hda6-7* mutant and in a rescued *hisn6a-2* mutant line now harboring active *HISN6B* alleles. Actin reactions served as loading controls. Reactions omitting reverse transcriptase (no RT) served as controls for genomic DNA contamination. (*D*) Mendelian segregation of hypomethylated *HISN6B* epialleles. F2 progeny of *hisn6a-2* × *hda6-7* were assayed for the presence (red) or absence (gray) of cytosine methylation at the HpaII/MspI restriction site of *HISN6A/B* promoters. The percentage of plants in each category is plotted (n = 32). Unlike *HISN6B*, *HISN6A* did not show significant levels of promoter methylation (Fig. S3 *A* and *C*).
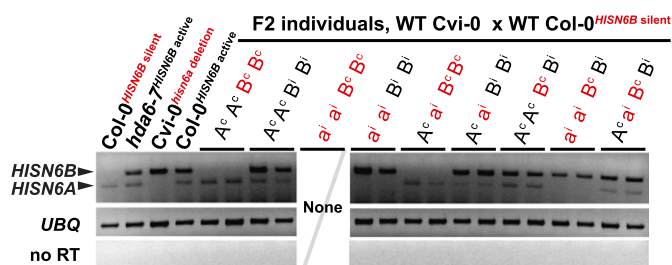
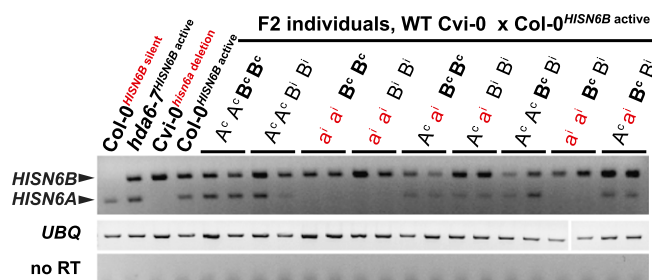**Fig. 3.** Active *HISN6B* epialleles circumvent lethality in *A. thaliana* Cvi-0 x Col-0 hybrids. (*A*) Schematic diagram of hybrid incompatibility between *A. thaliana* ecotypes Col-0 and Cvi-0. The red "a^i" indicates Cvi-0 *hisn6a* deletion alleles, the red "B^c" indicates silent Col-0 *HISN6B*, and the black "A^c" and "B^i" indicate active Col-0 *HISN6A* and Cvi-0 *HISN6B*, respectively. Note that alleles inherited from Col-0 carry the superscript "c", and alleles from Cvi-0 carry the superscript "i". All combinations of *HISN6A* and *HISN6B* alleles result in viable plants, except the double-homozygous combination of Cvi-0 *hisn6a* alleles (a^{i}a^i) and Col-0 *HISN6B* alleles (B^{c}B^c). (*B*) F2 genotypes resulting from the cross: WT Cvi-0 × WT Col-0 (with silent *HISN6B*). A total of 229 individuals were genotyped. Expected allele frequencies were calculated assuming Mendelian segregation. Comparison of observed to expected frequencies using Pearson's χ^2 test resulted in a *P* value of 4.8×10^{-8}, indicating hybrid incompatibility (arrow). (*C*) RT-PCR analysis of *HISN6A/B* gene expression in F2 progeny of the WT Cvi-0$^{hisn6a\ deletion}$ × WT Col-0$^{HISN6B\ silent}$ cross. Two individuals for each of the eight observed genotypes were assayed. Ubiquitin (*UBQ*) amplification products served as loading controls. Reactions without reverse transcriptase (no RT) served as controls for DNA contamination. Col-0$^{HISN6B\ silent}$, Cvi-0$^{hisn6a\ deletion}$, *hda6-7*, and Col-0 carrying reactivated *HISN6B* alleles served as *HISN6* expression controls. (*D*) The schematic depicts the genetic mechanism underlying rescue of hybrid compatibility following reanimation of Col-0 *HISN6B* alleles. The red "a^i" indicates Cvi-0 *hisn6a* deletion alleles, the black "B^c" indicates active Col-0 *HISN6B*, and the black "A^c" and "B^i" indicate active Col-0 *HISN6A* and Cvi-0 *HISN6B*, respectively. Note that alleles inherited from Col-0 carry the superscript "c", and alleles from Cvi-0 carry the superscript "i". All combinations of *HISN6A* and *HISN6B* alleles result in viable plants, including the previously lethal combination of two Cvi-0 *hisn6a* alleles (a^{i}a^i) and two Col-0 *HISN6B* alleles (B^{c}B^c). (*E*) F2 genotypes of progeny resulting from the cross of WT Cvi-0 × Col-0 (active *HISN6B*). Allele frequencies among 229 F2 individuals are shown. Expected allele frequencies were calculated assuming Mendelian segregation. Comparison of observed and expected statistics using Pearson's χ^2 test resulted in a *P* value of 0.78, indicating restored hybrid compatibility (arrow). (*F*) *HISN6A/B* expression in the F2 progeny of the Cvi-0$^{hisn6a\ deletion}$ × Col-0$^{HISN6B\ active}$ cross. Two individuals from each of the nine observed genotypes were assayed. *UBQ* reactions served as loading controls. The interruption in this panel corresponds to the end of one agarose gel row and the beginning of the next row. Reactions without reverse transcriptase (no RT) served as controls for DNA contamination. Col-0$^{HISN6B\ silent}$, Cvi-0$^{hisn6a\ deletion}$, *hda6-7*, and Col-0 carrying reactivated *HISN6B* served as controls.

plants expressed only *HISN6A*, and *hda6-7* mutants expressed both *HISN6A* and *HISN6B*, the viable *hisn6a-2* homozygotes expressed only *HISN6B* (Fig. 2*C*; *hisn6a-2*;*HISN6B* active).

We also crossed *hisn6a-2* (−/+) to the cytosine methyltransferase mutants *cmt3-11t* or *met1-7*. Viable *hisn6a-2* homozygotes represented 20% of the F2 plants resulting from the *cmt3-11t* cross and 11% of the F2 plants resulting from the *met1-7* cross (Fig. 2*B*). In contrast, crosses to *drm2-2* or *hda19-1t*, a histone deacetylase that is functionally distinct from HDA6 (42, 43), yielded no viable *hisn6a-2* homozygous F2 progeny (Fig. 2*B*). We conclude that *HISN6B* can be converted from a silent epiallele to an active allele in *hda6*, *cmt3*, or *met1* mutants, allowing the reanimated gene to rescue plants lacking the normally essential *HISN6A* gene.

Analysis of F2 individuals in the *hisn6a-2* (−/+) × *hda6-7* segregating population revealed *HISN6B* promoter methylation in 72% of the plants, consistent with a 3:1 ratio owing to Mendelian inheritance of methylated or unmethylated alleles (Fig. 2*D* and Fig. S3*A*). Because the unmethylated *HISN6B* allele segregated independently of the *hda6-7* mutation, we were able to identify an F3 line (Col-0^HISN6B active) that is homozygous for active *HISN6B* epialleles in an otherwise genetically WT background (Fig. 2*A*; F3 individual 82 in Fig. S3*B*). After self-fertilization of this line for three generations, no resetting to the silent, methylated state was observed (Fig. S3*C*); thus, this line, designated Col-0^HISN6B active, was used for further genetic comparisons to WT plants, designated Col-0^HISN6B silent, homozygous for silent, methylated *HISN6B* epialleles. Analysis of methylome data obtained by Schmitz et al. (44) showed that methylated *HISN6B* epialleles were stably inherited over a span of 30 generations (Fig. S3*D*).

In Cvi-0 × Col-0 F2 hybrids, homozygosity for both Col-0 *HISN6B* and Cvi-0 *hisn6a* is lethal (Fig. 3*A*) (31). We confirmed this among 229 Cvi-0^hisn6a deletion × Col-0^HISN6B silent F2 progeny, using PCR to detect Col-0 *HISN6A* (abbreviated A^c), Col-0 *HISN6B* (B^c), Cvi-0 *hisn6a* (a^i), and Cvi-0 *HISN6B* (B^i) alleles. Although ∼14 individuals (1/16) could be expected to have the genotype a^ia^i B^cB^c, none were observed (Fig. 3*B*, arrow), a significant deviation ($P = 4.8 \times 10^{-8}$, Pearson's χ^2 test) indicating hybrid incompatibility. Reverse-transcription–cleaved amplified polymorphic sequence (RT-CAPS) analyses revealed that hybrid individuals that are homozygous for WT Col-0 (B^cB^c) *HISN6B* alleles failed to express *HISN6B*, whereas individuals that inherited at least one *HISN6B* allele from Cvi-0 (B^i or B^iB^i) showed *HISN6B* expression (Fig. 3*C*). This indicates that silent or active *HISN6B* alleles of the parental ecotypes are faithfully transmitted. The promoter methylation marks of Col-0 *HISN6B* (B^c) alleles were also faithfully inherited among F2 hybrid individuals (Fig. S4*A*).

We next tested whether derepression of Col-0 *HISN6B* alleles would now allow the survival of F2 hybrids homozygous for both Col-0 *HISN6B* and Cvi-0 *hisn6a* (Fig. 3*D*). Indeed, the Cvi-0^hisn6a deletion × Col-0^HISN6B active cross yielded 17 healthy a^ia^i B^cB^c individuals in an F2 population of 229 plants (Fig. 3*E*), which is statistically indistinguishable from the expected ∼14 plants ($P = 0.78$, Pearson's χ^2 test). Col-0 *HISN6B* allele expression in the F2s (Fig. 3*F*) correlates with the near absence of *HISN6B* methylation (Fig. S4*B*). Collectively, these genetic tests show that reversion of *HISN6B* epialleles from a methylated, silent state to a hypomethylated, active state eliminates *HISN6*-based hybrid incompatibility between the Col-0 and Cvi-0 ecotypes of *A. thaliana*.

Discussion

Our study shows that ecotype-specific silencing of duplicated *HISN6* genes occurs in *A. thaliana* and is maintained by symmetric CG and CHG methylation involving HDA6, MET1, and CMT3. MET1- and CMT3-dependent DNA methylation can maintain silent epialleles over numerous meiotic generations, independently of initial silencing signals (16, 17, 22–24, 45). Mutation of *MET1*, *CMT3*, or *HDA6* converts silent *HISN6B* epialleles into active,

unmethylated alleles that are stably transmitted according to Mendelian rules of segregation. Moreover, reactivation of *HISN6B* circumvents the normal lethality of *hisn6a* mutations in Col-0 and prevents the occurrence of *HISN6* allele-dependent hybrid lethality among Cvi-0 × Col-0 hybrid progeny.

Hybrid incompatibility involving *HISN6A* and *HISN6B* alleles fits the model of Lynch and Force in that alternative *HISN6A* vs. *HISN6B* expression states lead to deleterious gene combinations in Cvi-0 × Col-0 F2 progeny (7, 31). Unlike the model of Bateson, Dobzhansky, and Muller, the Lynch and Force model for hybrid incompatibility does not require gene neofunctionalization; instead, differential loss of function of one member of a duplicated gene pair in different subpopulations or ecotypes spawns incompatibilities if the ecotypes hybridize. Examples in plants include the *DPL1* and *DPL2* genes of *Oryza sativa* subspecies *indica* and *japonica* (46), and the *AtFOLT1* and *AtFOLT2* genes of *A. thaliana* (29). The latter report showed that Col-0 × C24 and Col-0 × Sha incompatibilities correlate with the duplication, and additional complex rearrangement, of *AtFOLT1* in the C24 and Sha ecotypes. These mutations trigger methylation of *AtFOLT1*, leaving *AtFOLT2* as the sole active copy in C24 or Sha and causing hybrid incompatibility with Col-0, which lacks *AtFOLT2* altogether. Our study demonstrates that transgenerationally heritable (but fully revertible) epialleles that have not undergone inverted duplication, rearrangement, or mutation also contribute to hybrid incompatibility, providing additional evidence that epigenetic variation can foster reproductive isolation (29, 47, 48) in a manner consistent with the hypothesis of Lynch and Force.

Materials and Methods

Plant Materials. The *A. thaliana* ecotype Col-0 used in this study was a laboratory stock of the C.S.P. laboratory. Ecotype Cvi-0 (CS22614) was obtained from the Arabidopsis Biological Resource Center at Ohio State University. The *hda6-6* (*axe1-5*) and *hda6-7* (*rts1-1*) mutants were described by Murfett et al. (38) and Aufsatz et al. (37). *hda19-1t* is the *athd1-t1* (Ws) mutant allele of Tian et al. (42) introgressed into Col-0 by three backcrosses. The RNA polymerase mutants *pol IV* (*nrpd1-3*) and *pol V* (*nrpe1-11*) were described by Onodera et al. (49) and Pontes et al. (2006) (50). The mutants *drm2-2*, *cmt2-3* (SALK_012874), *cmt3-11t* (SALK_148381), *hisn6a-2* (SAIL_750), and *hisn6a-3* (SALK_089516), and the triple mutant *drm1-2 drm2-2 cmt3-11t*, were obtained from the Arabidopsis Biological Resource Center. *met1-3* was described by Saze et al. (16), and *met1-7* (SALK_076522) was obtained from the Nottingham Arabidopsis Stock Center.

RNA Analyses. Total RNA was extracted from 2-wk-old rosettes or from inflorescences using TRI Reagent (Molecular Research Center). For semiquantitative RT-PCR, 1.5 μg of DNase I-treated total RNA was used for random-primed cDNA synthesis by SuperScript III reverse transcriptase (Invitrogen). Standard PCR was performed on cDNA aliquots (∼100 ng of RNA input) using GoTaq Green (Promega) and the primers listed in Table S1. PCR products were analyzed either directly by agarose gel electrophoresis (*Actin* and *UBQ* controls) or following restriction enzyme digest (RsaI) and then agarose gel electrophoresis (RT-CAPS for *HISN6A/B*).

DNA Analyses. For genotyping, genomic DNA was purified from 2-wk-old seedlings using a CTAB extraction protocol. GoTaq Green Master Mix (2×; Promega) was mixed with ∼100 ng of genomic DNA and particular genotyping primer pairs. PCR products were scored either directly by agarose gel electrophoresis or following restriction enzyme digest (BspHI) and then agarose gel electrophoresis (CAPS). For DNA methylation analyses, genomic DNA was isolated from inflorescence tissue using the Nucleon PhytoPure DNA extraction kit (Amersham). Chop PCR assays were performed using 100 ng of restriction enzyme-digested ("chopped") genomic DNA as in Earley et al. (51). Primers used for genotyping and Chop PCR are listed in Table S1.

Bioinformatic Analyses. Analysis of WT and mutant methylomes of ecotype Col-0 (Fig. 1*E* and Fig. S2*C*) were performed on data from the National Center for Biotechnology Information (NCBI) Gene Expression Omnibus (GEO) accession no. GSE39901 (six datasets, wiggle format) (40). Methylation profiles were based on *HISN6A* gene model AT5G10330.8 and *HISN6B* gene model AT1G71920.2 (Araport11), whose similar intron/exon structures facilitated

comparison of the two genes. Fractional cytosine methylation in CG, CHG, and CHH sequence contexts were converted from wiggle to bigWig format, extracted using the bwtool software, and then plotted in Microsoft Excel (52). For the comparison of *A. thaliana* ecotype methylomes (Fig. 1*G* and Fig. S2*E*), datasets were obtained from NCBI GEO accession no. GSE43857 (927 ecotype datasets, tabular format) (41). After removing redundant or unidentified ecotypes, 892 methylomes remained for analysis. For each methylome, CG, CHG, and CHH methylation were tallied separately over 100-bp nonoverlapping windows in *HISN6A* or *HISN6B*, respectively, starting 500 bp upstream of the transcription start site (+1) and stopping 300 bp downstream of the transcription termination site (TTS). Hierarchical clustering was then performed using Euclidean distance and Ward's method to regroup ecotypes with similar patterns of cytosine methylation along *HISN6A* or *HISN6B*. Heatmaps were drawn using the "heatmap.2" function of R. For *HISN6B*, ecotypes were assigned to two visually evident categories: methylated promoter versus unmethylated promoter.

Statistical Tests. Chi-square goodness-of-fit tests were performed on genotype data shown in Fig. 3 *B* and *E* to test the hypothesis of *HISN6B* methylation-dependent hybrid incompatibility and generate *P* values in each case. The GPower software (53) estimated that sample sizes of at least 158 F2 plants would be needed to determine whether the observed allele frequencies deviate from Mendelian expectations, a number far exceeded by the 229 F2 plants genotyped in each experiment.

1. Chae E, et al. (2014) Species-wide genetic incompatibility analysis identifies immune genes as hot spots of deleterious epistasis. *Cell* 159(6):1341–1351.
2. Bomblies K, et al. (2007) Autoimmune response as a mechanism for a Dobzhansky-Muller-type incompatibility syndrome in plants. *PLoS Biol* 5(9):e236.
3. Maheshwari S, Barbash DA (2011) The genetics of hybrid incompatibilities. *Annu Rev Genet* 45:331–355.
4. Bateson W (1909) Heredity and variation in modern lights. *Darwin and Modern Science*, ed Seward AC (Cambridge Univ Press, Cambridge, UK), pp 85–101.
5. Dobzhansky T (1936) Studies on hybrid sterility, II: Localization of sterility factors in *Drosophila* pseudo-obscura hybrids. *Genetics* 21(2):113–135.
6. Muller HJ (1942) Isolating mechanisms, evolution and temperature. *Biol Symp* 6:71–125.
7. Lynch M, Force AG (2000) The origin of interspecific genomic incompatibiity via gene duplication. *Am Nat* 156:590–605.
8. Lynch M, Conery JS (2000) The evolutionary fate and consequences of duplicate genes. *Science* 290(5494):1151–1155.
9. Gossmann TI, Schmid KJ (2011) Selection-driven divergence after gene duplication in *Arabidopsis thaliana*. *J Mol Evol* 73(3-4):153–165.
10. Han MV, Demuth JP, McGrath CL, Casola C, Hahn MW (2009) Adaptive evolution of young gene duplicates in mammals. *Genome Res* 19(5):859–867.
11. Cubas P, Vincent C, Coen E (1999) An epigenetic mutation responsible for natural variation in floral symmetry. *Nature* 401(6749):157–161.
12. Jacobsen SE, Meyerowitz EM (1997) Hypermethylated SUPERMAN epigenetic alleles in *Arabidopsis*. *Science* 277(5329):1100–1103.
13. Manning K, et al. (2006) A naturally occurring epigenetic mutation in a gene encoding an SBP-box transcription factor inhibits tomato fruit ripening. *Nat Genet* 38(8):948–952.
14. Martin A, et al. (2009) A transposon-induced epigenetic change leads to sex determination in melon. *Nature* 461(7267):1135–1138.
15. Blevins T, et al. (2014) A two-step process for epigenetic inheritance in *Arabidopsis*. *Mol Cell* 54(1):30–42.
16. Saze H, Mittelsten Scheid O, Paszkowski J (2003) Maintenance of CpG methylation is essential for epigenetic inheritance during plant gametogenesis. *Nat Genet* 34(1):65–69.
17. Chen W, et al. (2015) Requirement of CHROMOMETHYLASE3 for somatic inheritance of the spontaneous tomato epimutation Colourless non-ripening. *Sci Rep* 5:9192.
18. Lippman Z, May B, Yordan C, Singer T, Martienssen R (2003) Distinct mechanisms determine transposon inheritance and methylation via small interfering RNA and histone modification. *PLoS Biol* 1(3):E67.
19. Jeddeloh JA, Stokes TL, Richards EJ (1999) Maintenance of genomic methylation requires a SWI2/SNF2-like protein. *Nat Genet* 22(1):94–97.
20. Kankel MW, et al. (2003) *Arabidopsis* MET1 cytosine methyltransferase mutants. *Genetics* 163(3):1109–1122.
21. Mittelsten Scheid O, Afsar K, Paszkowski J (1998) Release of epigenetic gene silencing by trans-acting mutations in *Arabidopsis*. *Proc Natl Acad Sci USA* 95(2):632–637.
22. Lindroth AM, et al. (2001) Requirement of CHROMOMETHYLASE3 for maintenance of CpXpG methylation. *Science* 292(5524):2077–2080.
23. Bartee L, Malagnac F, Bender J (2001) *Arabidopsis* cmt3 chromomethylase mutations block non-CG methylation and silencing of an endogenous gene. *Genes Dev* 15(14):1753–1758.
24. Quadrana L, Colot V (2016) Plant transgenerational epigenetics. *Annu Rev Genet* 50:467–491.
25. Teixeira FK, et al. (2009) A role for RNAi in the selective correction of DNA methylation defects. *Science* 323(5921):1600–1604.
26. Matzke MA, Aufsatz W, Kanno T, Mette MF, Matzke AJ (2002) Homology-dependent gene silencing and host defense in plants. *Adv Genet* 46:235–275.
27. Wendte JM, Pikaard CS (2017) The RNAs of RNA-directed DNA methylation. *Biochim Biophys Acta* 1860(1):140–148.
28. Matzke MA, Mosher RA (2014) RNA-directed DNA methylation: An epigenetic pathway of increasing complexity. *Nat Rev Genet* 15(6):394–408.
29. Durand S, Bouché N, Perez Strand E, Loudet O, Camilleri C (2012) Rapid establishment of genetic incompatibility through natural epigenetic variation. *Curr Biol* 22(4):326–331.
30. Bender J, Fink GR (1995) Epigenetic control of an endogenous gene family is revealed by a novel blue fluorescent mutant of *Arabidopsis*. *Cell* 83(5):725–734.
31. Bikard D, et al. (2009) Divergent evolution of duplicate genes leads to genetic incompatibilities within *A. thaliana*. *Science* 323(5914):623–626.
32. Muralla R, Sweeney C, Stepansky A, Leustek T, Meinke D (2007) Genetic dissection of histidine biosynthesis in *Arabidopsis*. *Plant Physiol* 144(2):890–903.
33. Ingle RA (2011) Histidine biosynthesis. *Arabidopsis Book* 9:e0141.
34. Berr A, et al. (2006) Chromosome arrangement and nuclear architecture but not centromeric sequences are conserved between *Arabidopsis thaliana* and *Arabidopsis lyrata*. *Plant J* 48(5):771–783.
35. Schmickl R, Jørgensen MH, Brysting AK, Koch MA (2010) The evolutionary history of the *Arabidopsis lyrata* complex: A hybrid in the amphi-Beringian area closes a large distribution gap and builds up a genetic barrier. *BMC Evol Biol* 10:98.
36. Moore RC, Purugganan MD (2003) The early stages of duplicate gene evolution. *Proc Natl Acad Sci USA* 100(26):15682–15687.
37. Aufsatz W, Mette MF, van der Winden J, Matzke M, Matzke AJ (2002) HDA6, a putative histone deacetylase needed to enhance DNA methylation induced by double-stranded RNA. *EMBO J* 21(24):6832–6841.
38. Murfett J, Wang XJ, Hagen G, Guilfoyle TJ (2001) Identification of *Arabidopsis* histone deacetylase HDA6 mutants that affect transgene expression. *Plant Cell* 13(5):1047–1061.
39. Law JA, Jacobsen SE (2010) Establishing, maintaining and modifying DNA methylation patterns in plants and animals. *Nat Rev Genet* 11(3):204–220.
40. Stroud H, Greenberg MV, Feng S, Bernatavichute YV, Jacobsen SE (2013) Comprehensive analysis of silencing mutants reveals complex regulation of the *Arabidopsis* methylome. *Cell* 152(1-2):352–364.
41. Kawakatsu T, et al.; 1001 Genomes Consortium (2016) Epigenomic diversity in a global collection of *Arabidopsis thaliana* accessions. *Cell* 166(2):492–505.
42. Tian L, et al. (2003) Genetic control of developmental changes induced by disruption of *Arabidopsis* histone deacetylase 1 (AtHD1) expression. *Genetics* 165(1):399–409.
43. Gao MJ, et al. (2015) SCARECROW-LIKE15 interacts with HISTONE DEACETYLASE19 and is essential for repressing the seed maturation programme. *Nat Commun* 6:7243.
44. Schmitz RJ, et al. (2011) Transgenerational epigenetic instability is a source of novel methylation variants. *Science* 334(6054):369–373.
45. Mathieu O, Reinders J, Caikovski M, Smathajitt C, Paszkowski J (2007) Transgenerational stability of the *Arabidopsis* epigenome is coordinated by CG methylation. *Cell* 130(5):851–862.
46. Mizuta Y, Harushima Y, Kurata N (2010) Rice pollen hybrid incompatibility caused by reciprocal gene loss of duplicated genes. *Proc Natl Acad Sci USA* 107(47):20417–20422.
47. Lafon-Placette C, Köhler C (2015) Epigenetic mechanisms of postzygotic reproductive isolation in plants. *Curr Opin Plant Biol* 23:39–44.
48. Richards EJ (2006) Inherited epigenetic variation: Revisiting soft inheritance. *Nat Rev Genet* 7(5):395–401.
49. Onodera Y, et al. (2005) Plant nuclear RNA polymerase IV mediates siRNA and DNA methylation-dependent heterochromatin formation. *Cell* 120(5):613–622.
50. Pontes O, et al. (2006) The *Arabidopsis* chromatin-modifying nuclear siRNA pathway involves a nucleolar RNA processing center. *Cell* 126(1):79–92.
51. Earley KW, et al. (2010) Mechanisms of HDA6-mediated rRNA gene silencing: Suppression of intergenic Pol II transcription and differential effects on maintenance versus siRNA-directed cytosine methylation. *Genes Dev* 24(11):1119–1132.
52. Pohl A, Beato M (2014) bwtool: A tool for bigWig files. *Bioinformatics* 30(11):1618–1619.
53. Faul F, Erdfelder E, Lang AG, Buchner A (2007) G*Power 3: A flexible statistical power analysis program for the social, behavioral, and biomedical sciences. *Behav Res Methods* 39(2):175–191.